J. Physiol. (1981), **314**, *pp.* 565–593
With 15 text-figures
Printed in Great Britain

MEMBRANE CHARGE MOVEMENT IN CONTRACTING AND NON-CONTRACTING SKELETAL MUSCLE FIBRES

BY P. HOROWICZ AND M. F. SCHNEIDER

From the Department of Physiology, University of Rochester, School of Medicine and Dentistry, Rochester, New York 14642, U.S.A.

(*Received 27 February 1980*)

SUMMARY

1. The single gap voltage clamp technique (Kovács & Schneider, 1978) was used to monitor membrane charge movement in tendon-terminated short segments of cut frog skeletal muscle fibres.

2. Experiments were performed both on fibres able to contract and on fibres in which contraction was eliminated by exposing the open end to a solution containing 20 mM-EGTA. In both cases ionic conductances were minimized by using a predominantly caesium glutamate solution at the open end and a predominantly tetraethylammonium sulphate solution with tetrodotoxin at the closed end.

3. Modifications of previously used charge movement analysis procedures included synthesis of a 'mean linear' ON and OFF capacitative transient from the OFFs of several different hyperpolarizing pulses and use of only the first 35 msec of the 'mean linear' transient so that base lines could be fitted to unaltered latter parts of ON and OFF currents for depolarizing pulses.

4. Simultaneous two-micro-electrode and gap current recording from gap-clamped fibres with blocked contraction established the validity of gap-recorded charge movement currents.

5. For pulses to below about 0 mV in non-contracting fibres the charges Q_{ON} and Q_{OFF} moved by the non-linear transient currents at pulse ON and OFF were approximately equal. For pulses to between about 0 and +50 mV Q_{OFF} exceeded Q_{ON}, with the charge inequality increasing with both pulse amplitude and pulse duration.

6. Use of 20 mM-cobalt in the solution at the closed end eliminated the ON:OFF charge inequality for large depolarizations by decreasing Q_{OFF}.

7. The charge inequality and cobalt effect indicate that, in the absence of cobalt, ionic conductance was being slowly activated during depolarizations to between 0 and +50 mV and that inward calcium current tails were contributing to the measured Q_{OFF} values. The small and slowly developing ionic current during large depolarizations was probably removed with the straight sloping base line so that Q_{ON} was minimally affected by conductance activation.

8. Average Q *vs.* V results for pulses to at most 0 mV in eighteen non-contracting fibres were well fitted by the two-state Boltzmann model where

0022-3751/81/4850-0819 $07.50

$Q = Q_{max}/[1+\exp-(V-\bar{V})/k]$ with $Q_{max} = 26{\cdot}7 \pm 0{\cdot}6$ nC/μF, $k = 16{\cdot}7 \pm 0{\cdot}6$ mV and $\bar{V} = -32{\cdot}9 \pm 1{\cdot}0$ mV (least-squares values ± S.D. obtained from fit).

9. In contracting fibres the only apparent artifact produced by contraction in the I_Q records for pulses to at most 0 mV was a 'bowing' of the OFF base lines for the larger pulses. The ON records appeared to be unaffected by contraction artifacts.

10. The average Q *vs.* V relationship for pulses to at most 0 mV in contracting fibres was virtually identical to the one obtained from fibres in which contraction was blocked.

11. The ON portions of I_Q records for pulses to between about -50 and -25 mV exhibited prolonged tails, plateaux or secondary rising phases whereas the OFF portions decayed smoothly. I_Q time courses were not noticeably different with or without blockage of contraction by internal EGTA.

INTRODUCTION

Skeletal muscle fibres have membrane currents that appear to arise from the movement of charged groups or the rotation of dipolar molecules within the fibre membrane (Schneider & Chandler, 1973; Chandler, Rakowski & Schneider, 1976*a*; Adrian & Almers, 1976). Such charge displacement currents occur over an appropriate voltage range and are sufficiently rapid for the movement of charged groups within the transverse (T-)tubular membrane to be the first step in the chain of events leading from T-tubule depolarization to calcium release from the sarcoplasmic reticulum (Schneider & Chandler, 1973). The fact that the charge movement process becomes refractory during prolonged depolarization and requires fibre repolarization for its reappearance (Chandler, Rakowski & Schneider, 1976*b*) may account for the partial or complete suppression of contractile activation by prolonged depolarization (Hodgkin & Horowicz, 1960) and is thus consistent with charge movement's playing a role in depolarization–contraction coupling. The time and voltage dependence of repriming of both charge movement and threshold contraction in depolarized fibres appear to be generally consistent with the charge movement hypothesis (Adrian, Chandler & Rakowski, 1976).

A severe limitation on previous attempts to relate charge movement to contractile activation has been that the charge movement measurements were carried out using internal micro-electrodes. In order to avoid fibre damage and artifacts of movement, contraction was generally blocked using either hypertonic solutions (Schneider & Chandler, 1973; Chandler *et al.* 1976*a*, *b*; Adrian & Almers, 1976) or pharmacological agents (Almers & Best, 1976; Almers, 1976). Alternatively, pulses were limited to those producing only just threshold movements of contracting fibres (Adrian *et al.* 1976).

In the present experiments we have largely overcome the previous limitation on fibre movement by using the single gap method developed by Kovács & Schneider (1978) for voltage-clamping a short segment of terminated muscle fibre. With the single gap system it has proved possible to record charge displacement currents for pulses to well beyond contraction thresholds in mechanically fully primed fibres in which depolarization–contraction coupling was not suppressed.

Since the fibres used in these experiments were cut at one end, modification of their

internal composition was also possible. In some experiments the cut fibre ends were exposed to relatively high concentrations of the calcium chelator EGTA, which eliminated contraction under isotonic conditions but appeared not to affect the charge displacement currents. This provided an opportunity to investigate the ionic and displacement currents accompanying large and long depolarizations in isotonic solutions without the use of other agents to block depolarization–contraction coupling. These experiments indicated that for pulses to positive membrane potentials the charge movement currents were contaminated by ionic currents, possibly through a calcium channel.

In this paper the procedures developed for measuring charge movement using the single gap system are presented. Charge movement is characterized both for contracting fibres in isotonic solutions without inhibitors of depolarization–contraction coupling and for non-contracting fibres in isotonic solutions in which contraction was blocked by internal EGTA. As far as could be determined, charge movement was essentially the same with or without contraction under these conditions. Several abstracts concerning various aspects of this work have previously been presented (Schneider & Horowicz, 1977, 1978, 1979).

METHODS

Fibre preparation and solutions

Experiments were carried out using semitendinosus or ileofibularis muscle fibre segments from frogs (*Rana pipiens*) which had been cold-adapted by a few days' to many weeks' refrigeration at about 5 °C. The procedures used for preparing cut fibres, mounting them in the single gap chamber and checking the Vaseline seal have been described by Kovács & Schneider (1978). In preparations used for this and the following paper (Horowicz & Schneider, 1981), the length l_C of intact terminated fibre segment extending beyond the gap ranged from 355 to 938 μm, its sarcomere length s ranged from 2·11 to 2·81 μm, and its width d in the plane perpendicular to the microscope axis ranged from 45 to 104 μm. The temperature ranged from 1 to 4 °C.

The solutions used at the open (pool A) and closed (pool C) fibre ends were designed to block most fibre membrane conductances; they are listed in Table 1. Low membrane conductances tend to minimize the potential decrement along the terminated segment and into the T-system and to remove ionic current components which might otherwise have obscured the charge displacement currents.

Electrical recording procedures

The membrane potential V_m and the longitudinal current I just beyond the gap in the intact fibre segment were monitored as the output signals V'_m and V'_I of a compensating circuit (Kovács & Schneider, 1978) which was adjusted by comparison with direct micro-electrode recording of V_m. Experiments were carried out at holding potentials V_H of about -100 mV. The actual value of V_H was measured as the change in potential on micro-electrode withdrawal after clamping V'_m at -100 mV, and was in all cases within a few millivolts of that value.

Previous analysis has shown that with the compensating circuit properly set, V'_m is an exact measure of V_m whereas V'_I has not been completely corrected for external gap current (Kovács & Schneider, 1978). To verify the validity of recording displacement currents using V'_I records, gap and micro-electrode recording were simultaneously carried out on several fibres. For these experiments one micro-electrode was inserted in the middle of the terminated segment to record voltage V_1 and a second micro-electrode was inserted just beyond the gap to record V_2. For the relatively short fibre lengths and low membrane conductances characteristic of these experiments, a very good approximation to the membrane current density per unit fibre length at the V_1 electrode is given by $8(V_2 - V_1)/3l_C^2 r_i$, where r_i is the internal resistance per unit length in the terminated segment (Adrian, Chandler & Hodgkin, 1970).

For the two-micro-electrode experiments, conducting silver paint shields were applied to within

about 1 mm of each electrode tip and then covered with an insulating coating (Valdiosera, Clausen & Eisenberg, 1974). Each shield was driven by the output of the unity-gain follower associated with the same electrode. This decreased the capacitance from each electrode barrel to ground. Without shielding, the capacitance to ground would have been relatively large, since relatively long lengths of electrode were under the virtually grounded pool C solution because of the small angle between each electrode and the horizontal.

TABLE 1. Composition of experimental solutions

	External solutions*					
	TEA	Cs	Rb	Co	SO_4	$CaSO_4$†
C1	150	0	10	0	80	7·2
C2	150	10	0	0	80	7·2
C3	125·4	10	0	20	87·7	7·5

	Internal solutions‡				
	Cs	Mg	Glutamate	Cl	EGTA
A1	120	2	120	4	1
A2	130	2	90	4	20

All concentrations are in mM. All solutions also contained 5 mM-Tris maleate buffer (pH 7·0).

* All external solutions contained 10^{-7} g/ml. tetrodotoxin.

† The total content of $CaSO_4$ is listed. The free Ca concentration was probably slightly less than 1 mM.

‡ Both internal solutions also contained 0·5 mM-ATP.

Maximum permissible contractions

Since the compensating circuit setting depended on the values of internal and external resistance across the gap, fibre movement in the gap during contraction would tend to introduce movement artifacts into the V'_m and V'_I recordings. The following measures were taken to minimize movement artifacts. (i) Fibres were generally mounted using a long length of tendon as a flexible lever so that large amounts of shortening could occur with minimal movement at the gap. (ii) In order to stabilize the fibre and gap geometry before setting the compensating circuit many fibres were repolarized and stimulated to produce well-suprathreshold movements. The fibres were then slowly depolarized without activating contraction, after which the compensating circuit was set and the fibre voltage-clamped. (iii) Each fibre was carefully observed at the gap using the compound microscope at 400× and the maximum pulse amplitudes and durations were limited so that at most only a few sarcomeres moved into the gap during contraction.

Digital data recording and storage

Data were recorded, stored and processed using a laboratory computer (Digital Equipment Corp., PDP-8E) equipped with DEC tape and disc storage units. V'_I was amplified using a 3A9 plug-in unit (10 kHz band width) in a 565 oscilloscope (Tektronix) and other signals were amplified using instrumentation amplifier circuits (Analog Devices, AD520J). Each signal to be recorded was digitally integrated for 255 consecutive 1 msec intervals (Kovács & Schneider, 1978). The dead time for transfer and reset was 3 μsec at the start of each interval. In most experiments V'_m and V'_I were simultaneously monitored. In those experiments in which both gap and micro-electrode recording were employed, the signals V'_m, V'_I, V_2 and ΔV ($= V_2 - V_1$) were recorded in various pairs.

Pulse sequences

The basic pulse pattern used in most of these experiments was a depolarizing pulse followed by two hyperpolarizing pulses of the same duration but of exactly half amplitude. However, since hyperpolarizing pulses to beyond about −160 to −170 mV often caused irreversible increases in V'_I, depolarizing pulses to beyond about +20 mV were generally accompanied by three hyperpolarizing pulses of one third amplitude.

A sequence of different depolarizing and appropriate hyperpolarizing pulses was applied and the desired signals recorded. The sequence was repeated until a temporary on-line addition of pulses

indicated that an acceptable signal/noise ratio had been attained. Digital records for every individual pulse application were stored separately on tape during the experiment. Average records were later compiled for each type of pulse in a given sequence. All analyses were carried out using average records obtained from four or eight individual pulse applications.

The basic pulse duration used to measure charge movement was 100 msec. However, to avoid movement artifacts in contracting fibres and to minimize the amount of obscuring ionic current turned on by large depolarizations, pulse durations were generally shortened to 50 msec for test pulses to beyond about −20 and −10 mV. Other durations were employed in a few experiments investigating the effect of pulse duration on ON and OFF charge movement.

Charge movement analysis

The current I_Q attributed to intramembrane charge movement is the component of capacitative current which varies non-linearly with membrane potential. In order to isolate I_Q, the linear capacitative current was first subtracted from the average overall V_1' current records for each depolarizing pulse using a 'mean linear' capacitative current calculated from the hyperpolarizing pulse currents as described in detail in the Results section. Assuming that the voltage step at the input to the terminated segment was perfectly square and that only relatively slowly changing ionic currents were present, ionic current components were then removed by subtracting straight sloping base lines (see Appendix). After isolating I_Q, the charge Q moved by I_Q was determined by integrating each I_Q record.

Straight sloping ON base lines were fitted by least squares to points 51–100 from the start of each 100 msec pulse and OFF base lines were fitted to points 51–135 from the end of each 50 and 100 msec pulse. Each straight sloping base line was extended back to the preceding ON or OFF pulse edge and was subtracted from the measured current. The area under each remaining ON or OFF transient was calculated as the sum of the first fifty points from pulse ON or OFF.

ON records for 50 msec pulses were not corrected for sloping base lines because of the limited number of possible base-line points to be fitted. Ionic currents were removed from ON transients for 50 msec pulses by subtracting the mean value of the last ten points from each of the first forty points.

Results from different fibres were normalized by expressing I_Q or Q relative to the linear capacitance measured in the same fibre. This approach cancels both the geometric and calibration factors particular to that fibre and makes results from different fibres comparable. Furthermore, both Q and linear capacitance must be slightly scaled up by a correction factor to give values which would apply if there had been no potential decrement along the fibre (Appendix, eqn. (3 A)). Provided that the fibre space constant λ_C in the terminated segment was independent of voltage, the scale factor would be the same for Q and linear capacitance and would thus be removed by the normalization procedure.

Curve fitting

Non-linear least squares curve fitting of theoretical functions to experimental data was carried out using the procedure described by Scarborough (1966). Error estimates for the least-squares parameter values were calculated as described by Cleland (1967).

RESULTS

A. Experiments on non-contracting fibres

A series of control experiments was carried out on fibres exposed for at least 50 min to a 20 mM-EGTA-containing solution (A 2, Table 1) at their cut ends in pool A. No movement was detected in these fibres for 100 msec depolarizations to membrane potentials as high as +50 to +80 mV. In contrast, fibres exposed to 1 mM-EGTA-containing solution (A 1, Table 1) in pool A for several hours exhibited large movements for much smaller depolarizations in virtually all cases. The use of 20 mM-EGTA at the cut end thus provided a means of evaluating the gap method for recording charge movement in the absence of any possible interference from contraction artifacts.

Total capacitative charge transfer

The total charge transferred by the ON and OFF capacitative transients in a fibre exposed to 20 mM-EGTA at its cut end are presented in Fig. 1 as a function of V'_m during the pulse. The values were obtained for each pulse from average V'_I records of total current by fitting and subtracting straight sloping base lines and integrating the remaining current. For each pulse except the two largest depolarizations the charge carried by the ON and OFF transients was in good agreement. For the hyperpolarizing pulses the charge transferred varied linearly with pulse size. The slope of the straight line drawn through the values for hyperpolarizing pulses in Fig. 1 gives the ratio of charge transferred to change in V'_m, which defines the linear fibre capacitance.

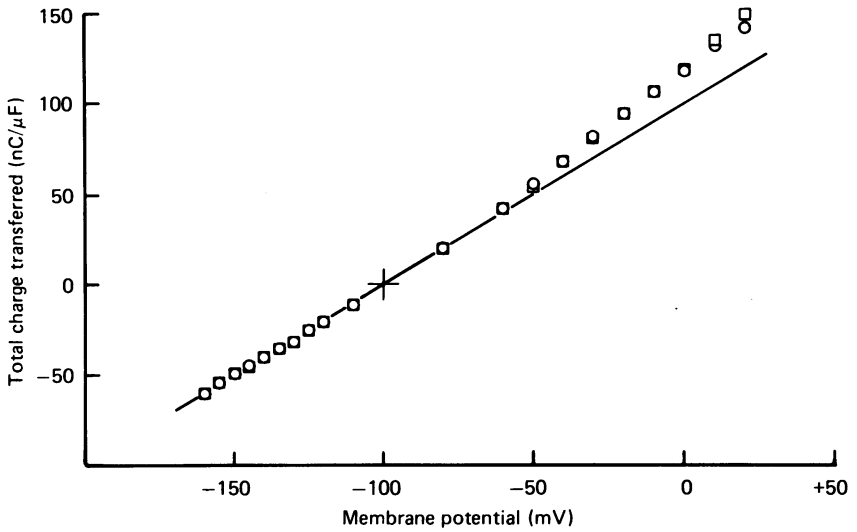

Fig. 1. Total capacitative charge transfer for hyperpolarizing and depolarizing pulses. Circles and squares give Q_{ON} and Q_{OFF}. Cross marks the holding potential. The straight line was drawn by eye through the points for hyperpolarizing pulses and defines the charge transfer via the fibre's linear capacitance. The ordinate scale was set so that the straight line corresponds to a charge transfer of 1 nC/μF of linear fibre capacitance for each millivolt change in membrane potential. Contraction was eliminated by using solution A2 at the open end. Fibre 75, run 3. $l_C = 482$ μm, $s = 2{\cdot}33$ μm, $d = 81$ μm. Temperature 2 °C.

Extending the line in Fig. 1 in the depolarizing direction gives the charge transfer predicted for the linear capacitance. Over almost the entire range of depolarizing pulses the actual charge transfer exceeded that predicted on the basis of the linear capacitance. The excess or non-linear component of capacitative charge transfer is that which is attributed to intramembrane charge movement.

Constructing a 'mean linear' capacitative transient

In order to examine the non-linear capacitative current in isolation, the linear capacitative current must be removed (Schneider & Chandler, 1973). In the present

experiments, current records from several different hyperpolarizing pulses were used to construct a 'mean linear' capacitative transient, which was then appropriately scaled and used to remove the linear capacitative current for each depolarizing pulse. Individual hyperpolarizing current records to be used for constructing the 'mean linear' transient are presented as *a–c* in Fig. 2. Such records often exhibited a slow decline in inward ionic current during the pulse, which was more pronounced the larger the hyperpolarization up to about −150 mV. In contrast, the OFF base lines were quite flat. To avoid possible errors due to improperly corrected ionic currents during the hyperpolarizing pulses, only the OFF currents were used for constructing the 'mean linear' transient.

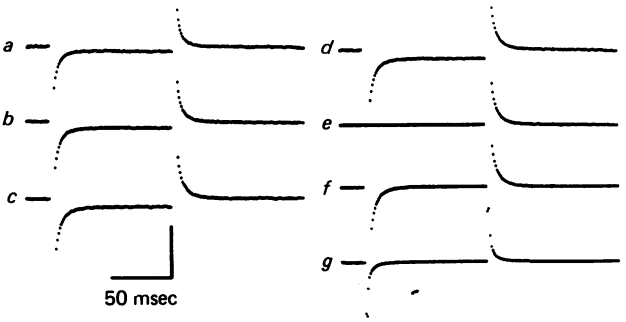

Fig. 2. Synthesis of a 'mean linear' capacitative transient from current records for hyperpolarizing pulses. Records *a–c* give total current for hyperpolarizing pulses of 20, 30 and 40 mV from a holding potential of −100 mV. Record *d*, the 'mean' hyperpolarizing current scaled to a 40 mV amplitude, was synthesized from *a* to *c* and similar records for 25 and 35 mV hyperpolarizing pulses as 40 $[(I_{20}/20+I_{25}/25+I_{30}/30+I_{35}/35+I_{40}/40)/5]$, where I_P is the current record for a hyperpolarizing pulse of amplitude P. Record *e* gives the OFF segment of *D* after subtracting sloping base lines. Record *f*, the 'mean linear' capacitative transient, was synthesized by using only the first thirty-five points of the OFF transient. These points were also inverted and put in the ON position. In order to display records *a–f* at this gain, initial points of the recorded transients were deleted. The number of initial ON and OFF points deleted was three in *a*, four in *b* and five in *c–f*. Record *g* is the same as *f* but displayed at lower gain with no points deleted. Here and in all other traces in this and the subsequent paper, each point gives the average value for a 1 msec interval. Vertical calibration is 2 μA/μF for *a–f* and 10 μA/μF for *g*. Horizontal calibration is 50 msec. Same fibre and run as in Fig. 1.

Signal-averaged currents for each 100 msec pulse to between about −120 and −140 or −150 mV in a given sequence were first divided by the change in V'_m during the pulse and then averaged (Fig. 2*d*). The mean OFF was corrected for ionic currents by fitting and subtracting a sloping base line. Since the current remaining after base-line subtraction declined to zero within 35 msec of pulse OFF (Fig. 2*e*), only the first 35 msec of the mean OFF transient were used, the remaining points being set equal to zero. The first thirty-five OFF points were also inverted and used as the first thirty-five points on the ON transient, so as to give a symmetric 'mean linear' capacitative transient (Fig. 2*f*). For use with 50 msec pulses, the 'mean linear' OFF was simply moved fifty locations towards the start of the pulse.

Using the 'mean linear' transient provided several advantages over using a

different hyperpolarizing pulse for each depolarizing pulse. It ensured that the voltage dependence of Q for depolarizing pulses was not influenced by any non-linearity of transient charge for hyperpolarizing pulses and that any inequality of Q_{ON} and Q_{OFF} must have had its origin in the transient currents for the depolarizing pulse. Since after the first 35 msec from pulse ON or OFF the 'mean linear' transient was set equal to zero, removal of linear capacitative current in no way obscured the determination of base-line currents for depolarizing pulses. Finally, averaging currents for several hyperpolarizing pulses minimized the noise introduced during removal of the linear capacitative current.

'Mean linear' capacitative transients were compiled separately for each sequence of pulses so that any drift in the preparation would affect the 'mean linear' and the nonlinear components equally.

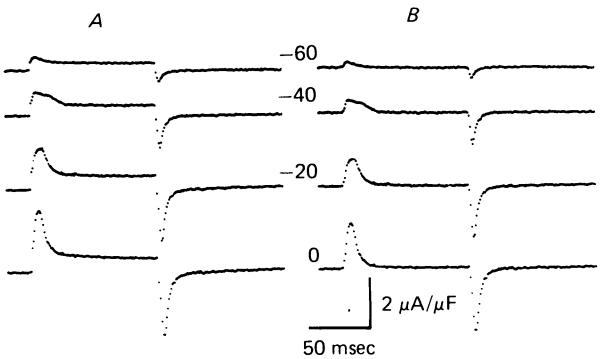

Fig. 3. Procedure for isolating charge movement currents. *A* and *B* give current records for pulses to the indicated membrane potentials (mV). *A*, total current plus appropriately scaled 'mean linear' capacitative current for hyperpolarizing pulses. *B*, records of *A* after fitting and subtracting straight sloping ON and OFF base lines. Same fibre and run as in Figs. 1 and 2.

Isolating charge movement currents

Linear capacitative currents were removed from the current record for each depolarizing pulse by multiplying the 'mean linear' transient by the depolarizing pulse step size and then adding the two currents. Resulting records of I_Q plus total ionic current for pulses to several potentials appear in column *A* of Fig. 3. The early transient during each ON is attributed to I_Q, whereas the slowly declining outward current seen later during the pulse, especially for the larger depolarizations, is assumed to be ionic. The OFF records show I_Q transients followed by relatively constant currents.

The records in column *B* of Fig. 3 give I_Q for the corresponding records in column *A* after removal of ionic current by subtraction of sloping base lines from each ON and OFF. These records resemble those reported for intact fibres (Schneider & Chandler, 1973; Chandler *et al.* 1976*a*; Adrian & Almers, 1976) in exhibiting non-first-order kinetics during the pulse, especially in the intermediate voltage range (Almers, Adrian & Levinson, 1975; Adrian & Peres, 1977), and relatively simple decay time courses at pulse OFF. Also as in intact fibres, the time course of the ON transient varied with pulse size whereas the OFF time course was similar for all pulses.

Equal and unequal ON and OFF non-linear charge transfer

A necessary characteristic for assigning non-linear currents such as those in Fig. 3*B* to intramembrane charge movement is the equality of the charge Q_{ON} moved outward during each pulse with the charge Q_{OFF} moved back inward following the pulse. The Q_{ON} and Q_{OFF} values obtained from the traces in Fig. 3*B* and from similar traces for pulses to other potentials in the same fibre are plotted in Fig. 4 as a function

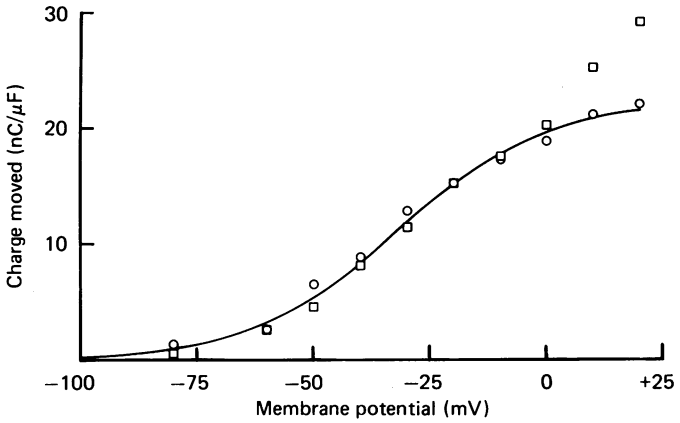

Fig. 4. Charge *vs.* voltage curve for a fibre with contraction abolished by high internal EGTA. Circles and squares give amounts of charge Q_{ON} and Q_{OFF} moved during the ON and OFF transients. The curve is the best fit of eqn. (1) to all points except the Q_{OFF} values for the three largest depolarizations. The parameter values (±1 S.D.) obtained from the curve fit were $Q_{max} = 22{\cdot}4 \pm 0{\cdot}7$ nC/μF, $k = 15{\cdot}7 \pm 1{\cdot}0$ mV and $\bar{V} = -32{\cdot}0 \pm 1{\cdot}4$ mV. Same fibre and run as in Figs. 1–3.

of membrane potential during the pulse. Over the negative range of membrane potentials Q_{ON} agreed quite well with Q_{OFF}, as required for intramembrane charge movement. However, as already noted in regard to Fig. 1, for pulses to and beyond about 0 mV there was a tendency of Q_{OFF} increasingly to exceed Q_{ON}. Similar charge inequalities have been observed for large depolarizations in intact fibres and have been attributed to contamination by delayed rectifier currents (Chandler *et al.* 1976*a*).

Time-dependent ionic currents contribute to non-linear charge transfer for large depolarizations

The inequality of Q_{ON} and Q_{OFF} observed with relatively large pulses (Fig. 4) was further investigated by studying the effect of pulse duration on charge movement. Three sets of current records from one such experiment are presented in Fig. 5, each set consisting of two ON and three OFF records for pulses to the same potential. The upper ON current record in each set is for a 120 msec pulse and was corrected only for linear capacitative current, whereas the lower one for the same pulse also had sloping base lines subtracted. The three OFF transients in each set were obtained using 30, 60 and 120 msec pulse durations and were corrected for both linear capacitative current and sloping base lines. For pulses to −16 mV the OFF transients

remained about constant for pulse durations of 30, 60 and 120 msec and the areas under the fully corrected ON and OFF transients were approximately equal. By contrast, for pulses to +44 mV the OFF transients increased with pulse duration and had noticeably greater areas than the ON transients. For pulses to +14 mV the growth of the OFF transient with pulse duration was less prominent.

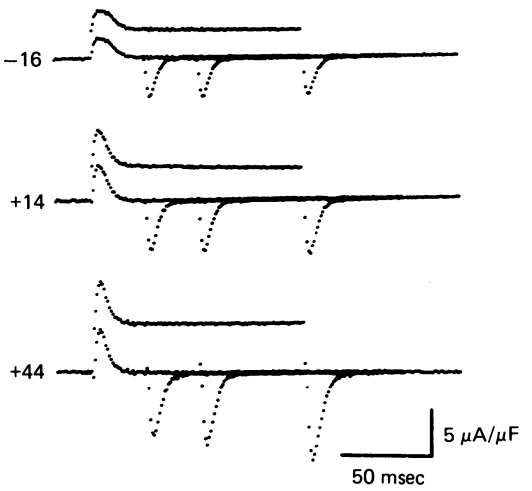

Fig. 5. Current due to non-linear charge transfer for large depolarizations of three durations. Each set of records was obtained using pulses to the indicated membrane potential (mV). In each set the upper record is the current for a 120 msec pulse with the 'mean linear' capacitative current removed but without base line subtraction. The lower records in each set give ON and OFF current records after removing both linear capacitative current and sloping base lines. Contraction was eliminated by solution A 2 at the open end. Fibre 83, runs 2 and 3. $l_C = 482\ \mu m$, $s = 2{\cdot}59\ \mu m$, $d = 68\ \mu m$. Temperature 3 °C.

The Q values obtained in this experiment are graphed as a function of pulse duration in Fig. 6. The open and filled symbols present Q_{ON} and Q_{OFF}, with each type of symbol corresponding to a different membrane potential. The lower continuous curve gives the time course of Q_{ON} for a 120 msec pulse to −16 mV, calculated as the running integral of I_Q, and the open circles situate Q_{ON} after 30, 60 and 120 msec. The last two values were necessarily equal since the sloping base lines were for this experiment fitted to the 61st–120th points during the pulse. The filled circles give the Q_{OFF} values for the pulses to −16 mV. The small increase in Q_{OFF} with increased pulse duration from 30 to 60 msec may be a true reflexion of the fact that Q_{ON} had not reached its final level in 30 msec at this potential. The further increase in pulse duration caused no further increase in Q_{OFF}. The Q_{ON} and Q_{OFF} values for all pulse durations at −16 mV were in fairly good agreement.

The upper continuous curve in Fig. 6 gives the Q_{ON} time course at +44 mV and demonstrates that at this potential all ON charge was moved in well under 30 msec. The Q_{ON} time course at +14 mV, which is given by the dashed curve in Fig. 6, was only slightly slower than the upper curve and was also completed in less than 30 msec.

Thus the Q_{ON} values for the two larger pulses (open squares and triangles in Fig. 6) were constant for the durations tested. Q_{ON} did become progressively larger with increased depolarization, although not in proportion to the pulse amplitude. In fact, there is a clear indication of near-saturation of Q_{ON} between +14 and +44 mV. For both of the larger pulses Q_{OFF} was substantially greater than Q_{ON}, and this inequality increased with pulse duration due to the growth of Q_{OFF}.

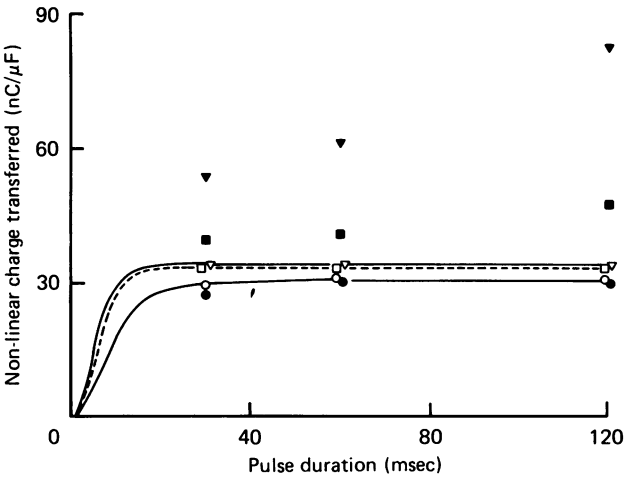

Fig. 6. Effect of pulse duration on ON and OFF non-linear charge transfer. The points give the amount of charge transferred by ON and OFF (open and filled symbols) non-linear current transients for pulses to −16 (○, ●), +14 (□, ■) and +44 (▽, ▼) mV, for the indicated durations. The lower (continuous), middle (dashed) and upper (continuous) curves give the time courses of Q_{ON} for the same respective pulses. All values were determined from the records in Fig. 5. Here and in other graphs in this and the subsequent paper some points may have been slightly displaced horizontally, but not vertically, so as to display superimposed points.

These results clearly raise the question of the nature of the measured non-linear charge transfer for these relatively large pulse amplitudes. The most likely explanation for the growth of the OFF transients with pulse duration is that one or more ionic conductances were being activated during the pulse in this range of potentials. Any relatively fast inward ionic current tail contributed by such conductances at pulse OFF would not have been removed by the sloping base-line correction and would have given rise to over-estimates of the OFF membrane charge movements. If the conductance were activated linearly with time during the pulse, as is indicated by the straight sloping base lines generally observed at potentials from 0 to +40 mV, the over-estimate of Q_{OFF} should have increased linearly with pulse duration, as was also observed.

The slope of the ON current component which varied linearly with time changed from negative to positive at a potential between about +40 and +50 mV, which is thus the net effective reversal potential for all time-dependent ionic currents. For pulses to beyond about +50 mV the net outward current after the initial capacitative surge was found to increase rapidly and in a non-linear manner with time. For such

pulses the non-linear capacitative currents could not be reliably separated by our methods from the ionic currents which occurred during the ON of the pulse, whereas for pulses to below about +50 mV the net outward current appears to have been accurately removed by subtracting sloping base lines.

It should be noted that more than one relatively slow conductance change was probably occurring during depolarizing pulses. For example, a slow linear decline in current was observed during pulses to negative membrane potentials (Fig. 3, −20 mV, and Fig. 5, −16 mV), but Q_{OFF} did not increase with pulse duration for such pulses (Fig. 5, −16 mV, and Fig. 6). This conductance change appears to be different from the conductance activated at positive potentials since any OFF ionic current tails which it produced must have been sufficiently slow to be removed with the sloping base line.

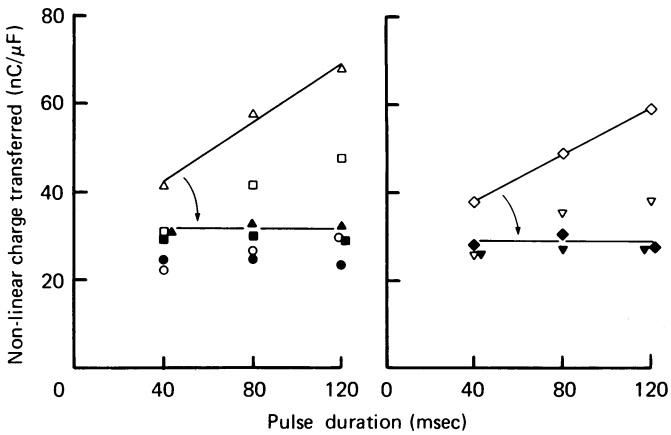

Fig. 7. Effect of external cobalt on non-linear charge transfer for large depolarizations of several durations. Open and filled symbols denote charge transferred by non-linear transient OFF currents with the 0 or 20 mM-cobalt in the external solution (C2 or C3, Table 1). Results obtained with pulses to +1 (○, ●), +21 (□, ■), +41 (△, ▲), +11 (▽, ▼) and +31 (◇, ◆) mV. The straight lines were drawn by eye through the points for the largest depolarization in each panel and the arrow indicates the change produced by cobalt for these pulses. Contraction was eliminated by solution A 2 at the open end. Fibre 119, cobalt-free results average of runs 2 and 9, cobalt-containing results run 6. l_C = 710 μm, s = 2·76 μm, d = 55 μm. Temperature 2 °C.

Ionic current contamination of charge movement at large depolarizations is decreased by external cobalt

In an attempt to block the ionic current contaminating the charge movement measurements for large depolarizations, charge movements were measured in the presence and absence of 20 mM-cobalt. Q_{OFF} values for the two conditions are plotted as a function of pulse duration in Fig. 7. In the absence of cobalt (open symbols) Q_{OFF} increased with pulse duration whereas in the presence of 20 mM-cobalt (filled symbols) the OFF transients became independent of pulse duration. The cobalt effect was reversible; in this experiment the growth of Q_{OFF} with pulse duration was found to be somewhat larger following return from the cobalt-containing solution than during the initial pre-cobalt measurements.

The values of Q_{ON} and Q_{OFF} obtained for the fibre of Fig. 7 in other runs using 100 msec pulses to a variety of membrane potentials in the absence (open symbols) and presence (filled symbols) of 20 mM-cobalt are plotted in Fig. 8 as a function of V'_m during the pulse. For pulses which depolarized the fibre as much as to −11 mV, cobalt had little effect on Q_{ON} or Q_{OFF}. For pulses which brought V'_m to between −1 and +39 mV Q_{ON} was unaffected by cobalt whereas Q_{OFF} was markedly depressed

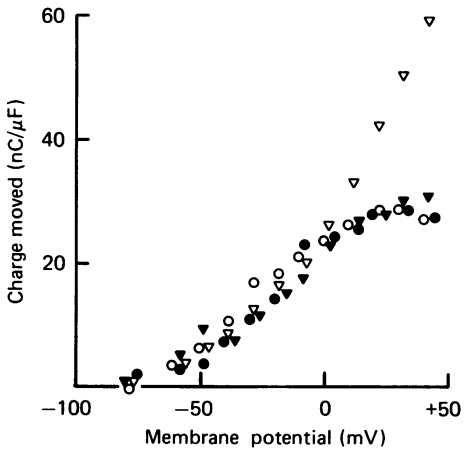

Fig. 8. Effects of external cobalt on the charge *vs.* voltage relationship. Open and filled symbols give results obtained with the fibre exposed to 0 or 20 mM-cobalt in the external solution. Each point gives the charge transferred by the non-linear transient current for the ON (circles) or OFF (triangles) of a 100 msec pulse. Cobalt-free results averaged from runs 1 and 8 and cobalt-containing results from run 5. Same fibre and conditions as in Fig. 7.

so that Q_{OFF} became approximately equal to Q_{ON}. This experiment indicates that 20 mM-cobalt had little effect on membrane charge movements while drastically reducing the ionic currents which contaminate the OFF I_Q records for large depolarizations.

The general conclusion from the pulse duration and cobalt experiments is that in the standard (cobalt-free) solutions used in these experiments, ON and OFF membrane charge movements were probably accurately measured over the negative range of membrane potentials. At positive potentials Q_{ON} may have been accurately determined but Q_{OFF} was over-estimated due to ionic current contamination. To avoid uncertain determinations no pulse to beyond about 0 mV was used in the rest of the experiments in this or the following paper.

Average charge movement at negative membrane potentials

Charge movement was measured at potentials ranging from about −80 to about 0 mV in 20 mV steps in eighteen fibres with cut ends exposed to the 20 mM-EGTA-containing solution. Average values of Q_{ON} (circles) and Q_{OFF} (triangles) from these fibres are presented in Fig. 9. For all but the largest depolarizations 100 msec pulses were used whereas for the largest depolarizations, which brought V'_m to about 0 mV, 100 msec pulses were used on six fibres and 50 msec pulses on the other twelve fibres.

Considering first the smaller pulses where ionic current presents no problem, at about −80, −60 and −20 mV the mean values on Q_{ON} and Q_{OFF} agreed essentially perfectly (Fig. 9). Ratios and differences of Q_{ON} and Q_{OFF} were calculated for each fibre at each membrane potential and their average values support the equality of Q_{ON} and Q_{OFF} at these potentials. At about −40 mV the mean value of Q_{ON} did appear to exceed slightly the mean Q_{OFF}, largely due to the results from two fibres

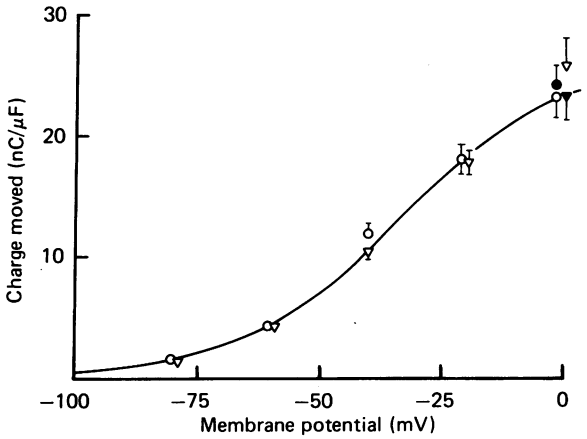

Fig. 9. Average charge *vs.* voltage curve for fibres with contraction eliminated by the relatively high EGTA-containing solution at the open end. Circles and triangles give mean values of Q_{ON} and Q_{OFF} for pulses to the indicated membrane potentials in eighteen fibres. Here and in subsequent graphs error bars give ±1 S.E.M. When no error bar is shown 1 S.E.M. is within the size of the symbol. Open symbols are for 100 msec pulses, the filled triangle is for 50 msec pulses and the filled circle is for 50 msec pulses and/or 100 msec ON records analysed for only 50 msec (see text). The curve is the best fit of eqn. (1) to results using the 100 msec Q_{ON} and 50 msec Q_{OFF} values at 0 mV and excluding the Q_{ON} and Q_{OFF} values for pulses to −40 mV in two fibres in which Q_{ON} was much larger than Q_{OFF} at −40 mV (see text). Parameter values (±1 S.D.) obtained from the fit were $Q_{max} = 26{\cdot}7 \pm 0{\cdot}6$ nC/μF, $k = 16{\cdot}7 \pm 0{\cdot}6$ mV and $\bar{V} = -32{\cdot}9 \pm 1{\cdot}0$ mV $355 \leqslant l_C \leqslant 811$ μm, $2{\cdot}13 \leqslant s \leqslant 2{\cdot}81$ μm, $47 \leqslant d \leqslant 104$ μm. Temperature 1–3 °C.

in which Q_{ON} was 58 and 76% larger than Q_{OFF}. For the other sixteen fibres the average percentage excess of Q_{ON} over Q_{OFF} at −40 mV was 9±5% (mean±S.E.M.). Excluding the values from these two fibres from the means at −40 mV decreased Q_{ON} by 6% but left Q_{OFF} unaltered. The Q_{ON} values for these two fibres thus appear to be excessively high.

For pulses to about 0 mV ionic current contamination of Q_{OFF} begins to be a problem, shown here by the mean Q_{OFF} being 10·5% larger for the fibres in which the 100 msec pulse was used than for those in which the 50 msec pulse was used (open *vs.* filled triangles at 0 mV in Fig. 9).

The excess Q_{OFF} for fibres in which 100 rather than 50 msec pulses to 0 mV were used cannot be attributed to a difference in the two groups of fibres since the average value of Q_{ON} calculated for each group agreed to within 1·4% of the overall mean when both the 50 and 100 msec ON I_Q records were analysed using the 50 msec ON analysis procedure without considering base line slope (see Methods). Since the two groups of fibres showed similar Q_{ON} values, the ON data provide an opportunity to evaluate the error introduced by ignoring base-line slope for 50 msec pulses to 0

mV. The filled circle at 0 mV gives the average of Q_{ON} values obtained from all eighteen fibres using the 50 msec ON analysis. The open circle gives the average Q_{ON} obtained using the sloping base-line correction on the I_Q records from the six fibres in which 100 msec pulses were used. At 0 mV the sloping base-line correction decreased the mean Q_{ON} to 96 % of the mean value obtained from the same I_Q records analysed for 50 msec without considering base-line slope.

The most accurate Q estimates at 0 mV are the 100 msec Q_{ON} value (open circle), from which the effects of slow ionic current were presumably eliminated by sloping base-line subtraction, and the Q_{OFF} value for the 50 msec pulses (filled triangle), which should be minimally contaminated by ionic current. Their good agreement may indicate that the ionic conductance activation during a 50 msec pulse at 0 mV was negligible. Alternatively, if the Q_{OFF} value could have been corrected for ionic current, it might have been found to be somewhat less than Q_{ON}.

The equation for a two-state Boltzmann system,

$$Q = Q_{max}/[1+\exp-(V-\bar{V})/k], \quad (1)$$

has previously been used to describe the steady-state Q *vs.* V relationship (Schneider & Chandler, 1973; Chandler *et al.* 1976*a*; Adrian & Almers, 1976). $\bar{V}$ defines the potential for 50 % charge movement, Q_{max} gives the maximum charge movement and the $1/k$ specifies steepness of the Q *vs.* V relationship. The curve in Fig. 9 is the best least-squares fit of eqn. (1) to the mean values of Q_{ON} and Q_{OFF}, using the 100 msec ON and 50 msec OFF values at 0 mV and excluding the two apparently high Q_{ON} values from the mean at −40 mV. The parameter values giving the best fit were 26·7 nC/μF for Q_{max}, 16·7 mV for k and −33 mV for $\bar{V}$. Since fibre-to-fibre differences in $\bar{V}$ might tend to broaden the average Q *vs.* V curve, eqn. (1) was also fitted to the values for each individual fibre; the results are given in Table 2. The means of the parameter values obtained from the individual fits (26·3 nC/μF for Q_{max}, 16·0 mV for k and −35 mV for $\bar{V}$) were in good agreement with those obtained by the fit to the mean data.

In five of the fibres Q values were also determined at about −50, −30, and −10 mV. Including these values in those fitted by eqn. (1) changed the Q_{max} and k values by a mean ± S.E. of only 3 ± 2 % and changed $\bar{V}$ by only 1 ± 1 mV. Q values determined at 20 mV increments from −80 to 0 mV thus appear to define fully the Q *vs.* V relationship over this interval.

For the two fibres in which Q_{ON} considerably exceeded Q_{OFF} at −40 mV, the fit was greatly improved when only the Q_{ON} value at −40 mV was excluded from the fit. The −40 mV Q_{OFF} value was then very close to the calculated Q *vs.* V curve. When only Q_{OFF} at −40 mV was excluded the fit was little improved and the −40 mV Q_{ON} value was well above the resulting curve. This further indicates that for these fibres the −40 mV Q_{ON} value was excessively high.

B. Experiments on contracting fibres

Fibres with cut ends exposed to 1 mM-EGTA-containing solution (A 1, Table 1) continued to contract during experiments lasting up to 4–5 hr. Although the strength of contraction appeared from visual observation to decline during long experiments, the contraction thresholds remained relatively stable, generally exhibiting only minor unsystematic drifts over periods up to several hours. Solution A 1 was thus used in pool A in order to study charge movement in fibres with maintained contractile activity.

TABLE 2. Parameter values giving best fits to steady-state charge *vs.* voltage data from fibres with contraction blocked by internal EGTA

(1)	(2)	(3)	(4)	(5)	(6)	(7)	(8)
		Q_{max} (nC/μF)		k (mV)		$\bar{V}$ (mV)	
Fibre	Run	Value	S.D.	Value	S.D.	Value	S.D.
75	3	20·3	0·6	13·6	0·8	−35	1
83	1	35·9	3·5	15·4	2·1	−35	4
116	2	31·7	3·9	19·9	2·7	−32	6
117*	1	26·3	1·9	14·7	1·6	−28	3
118	1	24·0	2·3	15·4	2·5	−37	4
119	1	22·2	2·4	12·8	2·8	−36	4
98	2	20·5	1·6	13·8	2·3	−34	3
99	1	48·8	6·8	19·0	3·5	−24	7
100*	2	29·1	1·4	13·9	1·5	−34	2
102	1	21·9	4·3	21·0	7·9	−44	12
103	1	20·0	1·3	12·8	2·1	−35	3
104	1	38·3	2·3	17·3	1·8	−34	3
106	1	24·8	1·3	14·3	1·7	−39	2
107	1	33·2	2·3	14·6	1·7	−28	3
109	1	17·7	3·8	19·8	6·7	−34	11
110	1	16·6	1·3	13·5	2·6	−40	4
111	1	21·6	3·0	17·0	5·1	−42	7
112	1	20·4	2·7	18·4	4·1	−36	7
Mean		26·3		16·0		−34·9	
±S.E.M.		±2·0		±0·6		±1·2	

Parameter values and estimates of their standard deviations (S.D.) obtained by least-squares fit of eqn. (1) to Q values measured at 20 mV increments from about −80 to 0 mV. For the upper group of six fibres the pulse to about 0 mV was 100 msec. The Q_{OFF} for this pulse was not considered for the fit (see text). For the lower group of twelve fibres the pulse to about 0 mV was 50 msec. The Q_{OFF} and 0·961 times the Q_{ON} for this pulse were used for the fit. All other pulses were 100 msec and both Q_{ON} and Q_{OFF} were used.

Means ± S.E.M. calculated with each individual value weighed in proportion to the inverse of its variance (= S.D. × S.D.), but with the weights for the two values with the smallest variances arbitrarily set equal to the weight of the value with the third smallest variance so as to avoid excessive emphasis on values of fibres with the very best fitted data, were 23·6 ± 0·3 nC/μF for Q_{max}, 14·9 ± 0·1 mV for k and −34·4 ± 0·2 mV for $\bar{V}$.

* The Q_{ON} value at about −40 mV in these fibres greatly exceeded Q_{OFF} and was not included in the fit.

Charge movement currents in contracting fibres

Fig. 10*A* presents I_Q records obtained from a contracting fibre using the standard procedure to eliminate linear capacitative current and sloping ON base lines. Detectable fibre movement was produced by the pulses to and beyond −37 mV. Aside from the bowed OFF base lines accompanying the relatively large contractions produced by the 100 msec pulse to −27 mV and the 50 msec pulses to −22 and −12 mV, the I_Q records from the contracting fibre in Fig. 10 are similar to those obtained from fibres in which movement was eliminated by high internal EGTA. The bowing of OFF base lines was relatively pronounced in this particular case due to the fact that only a relatively short tendon length was used in mounting the fibre.

When bowed OFF base lines were encountered, sloping base lines were not fitted to the OFF records. In these cases the average current measured from about 35–50 or 69 msec following pulse OFF was subtracted from each OFF point, with no correction made for time-dependent ionic current. Q_{OFF} values for such records were not considered in the analysis of the Q *vs.* V curve in contracting fibres.

In order to check for other possible movement artifacts the fibre in Fig. 10 was also studied using 20 mM-EGTA-containing solution (A 2) at its cut end. The marked

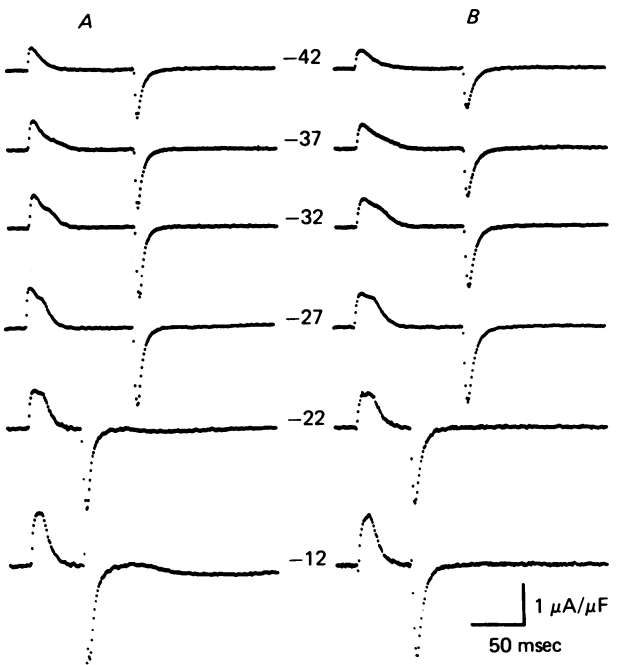

Fig. 10. Charge movement currents in the same fibre with contraction and after elimination of contraction by internal EGTA. Records in A and B give I_Q for pulses to the indicated membrane potentials. A, records obtained with the open end exposed to solution A 1. Movement was observed for all but the smallest pulse. Sloping OFF base lines were not used for the three largest pulses. B, records obtained after exposure of the open end to solution A 2 had eliminated contraction. No movement was observed and straight sloping base lines were removed from all transients. Fibre 76, runs 1 and 2 for A, 3 and 4 for B. $l_C = 760$ μm, $s = 2{\cdot}33$ μm, $d = 92$ μm. Temperature 1 °C for A and 2 °C for B.

bowing in the OFF base lines for pulses to and beyond −27 mV in the contracting condition (column A) was eliminated after exposure for 90 min to high internal EGTA had blocked contraction (column B). The fact that the bumps in the ON records were similar in the contracting and non-contracting conditions indicates that movement artifacts were not involved in producing the bumps. The small differences in amplitude and time course between the records in columns A and B are probably attributable to drift and slight differences in membrane potential, since I_Q time courses were quite sensitive to the pulse membrane potential. Similar results were obtained from a few other fibres studied in both 1 mM- and 20 mM-EGTA solutions.

The ON I_Q records from both contracting and non-contracting fibres exhibited prolonged tails, shoulders and bumps in the intermediate range of depolarizations. As mentioned above, Q_{ON} was also occasionally excessively high for similar depolarizations. The question therefore arose as to whether the tails, shoulders and bumps corresponded to a non-capacitative current component. The present results do not lend support to this possibility, since when the I_Q records were first grouped according to their ON shape, there was no difference in the mean values of Q_{ON}/Q_{OFF} from the group of smoothly decaying records compared with those from the groups with shoulders, with clear bumps or with flat tops.

Voltage dependence of charge movement is the same in contracting and non-contracting fibres

Fig. 11 presents Q *vs.* V data obtained from another fibre, first with the 1 mM-EGTA-containing solution (open symbols) and then following 105 min with the 20 mM-EGTA solution (filled symbols) at the cut end. Exposure of the cut end to 20 mM-EGTA for sufficient time totally to eliminate fibre contraction had essentially no effect on charge movement.

Fig. 12 presents average values of Q_{ON} (circles) and Q_{OFF} (triangles) for pulses to six different membrane potentials in sixteen contracting fibres. The open symbols denote values obtained using 100 msec pulses and the filled circles denote ON values for 50 msec pulses or for 100 msec pulses subjected to the 50 msec ON analysis. Due to base-line uncertainties in the presence of movement artifacts, Q_{OFF} values are not given for the two largest depolarizations in Fig. 12. For the other pulses Q_{ON} and Q_{OFF} were in close agreement. The curve in Fig. 12 is identical to the one in Fig. 9 and is the best fit of eqn. (1) to similar data obtained from non-contracting fibres. The voltage dependence of charge movement from -80 to 0 mV was clearly the same in contracting fibres as in fibres in which contraction had been abolished by using 20 mM-EGTA at their cut ends.

C. Micro-electrode recording from fibres voltage-clamped by the single gap method

Micro-electrode recording from fibres in which contraction had been eliminated by internal EGTA was used to evaluate several possible sources of error in the charge movement measurements made with the single gap method.

Gap- and micro-electrode-recorded charge movements

It has been shown that V_I' may over-estimate the actual steady-state fibre input current, even when the compensating circuit is perfectly adjusted (Kovács & Schneider, 1978). Since V_I' might also have been in error during transient currents, it was important to validate the I_Q records obtained using V_I'. The procedure adopted was to monitor simultaneously current by both the two-micro-electrode ΔV method (Adrian *et al.* 1970) and by V_I'. On the assumption that subtracting sloping base lines properly removed slow ionic current components from the ΔV records, the same analysis routine for isolating I_Q was applied to both micro-electrode and gap-current records. Currents recorded from one fibre using the two methods are given in Fig. 13. The currents obtained with each monitoring system were normalized to the linear capacitance determined using the same system so that the two sets of I_Q records in

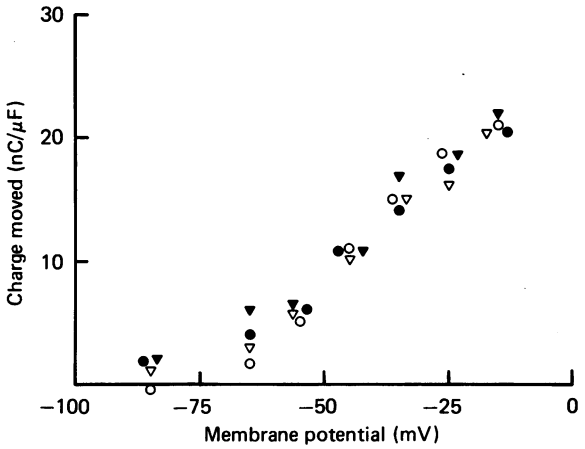

Fig. 11. Charge *vs.* voltage relationships for the same fibre before and after elimination of contraction by internal EGTA. Open symbols give results obtained in the contracting state with the open end exposed to solution A 1. Filled symbols give results obtained after contraction was eliminated by exposing the open end to solution A 2. Circles give Q_{ON} values and triangles give Q_{OFF}. Fibre 116, runs 1 (contracting) and 2 (non-contracting). $l_C = 634$ μm, $s = 2{\cdot}46$ μm, $d = 61$ μm. Temperature 2 °C.

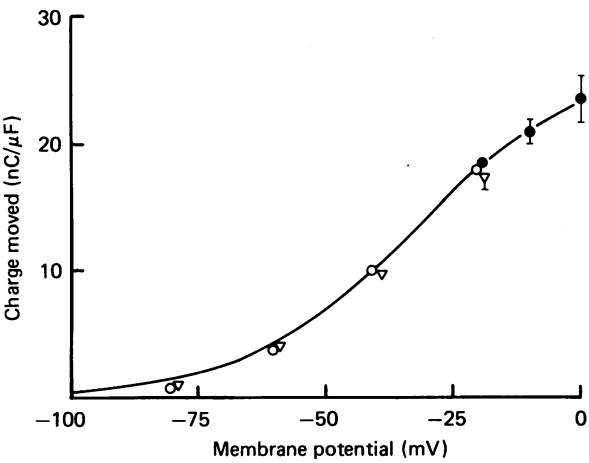

Fig. 12. Average charge *vs.* voltage relationship in contracting fibres. Average results from sixteen fibres. The symbols have the same significance as in Fig. 9. The 100 msec pulse values at −20 mV were obtained from only eight fibres and the 50 msec Q_{ON} values at −10 and 0 mV were obtained from only eleven and six fibres respectively. The curve is redrawn from Fig. 9. Measurements of charge moved during pulse durations producing just-detectable contraction for fourteen of these fibres are presented in Fig. 5 of the following paper. $380 \leqslant l_C \leqslant 938$ μm, $2{\cdot}11 \leqslant s \leqslant 2{\cdot}76$ μm, $45 \leqslant d \leqslant 92$ μm. Temperature 1–3 °C.

Fig. 13 correspond to the same relative scale. Apart from the greater noise in ΔV, the time courses of the ΔV (right) and V_I' (left) records of I_Q in Fig. 13 were similar for every pulse used. The amplitude of each normalized I_Q monitored by ΔV was, however, slightly larger than the corresponding I_Q monitored by V_I'.

The ratio of the charge movement recorded using ΔV to the charge movement recorded using V_I' was evaluated in three fibres for pulses to several membrane potentials. Before taking the ratios, Q for each method was normalized to the linear capacitance determined using the same method so as to cancel the correction terms

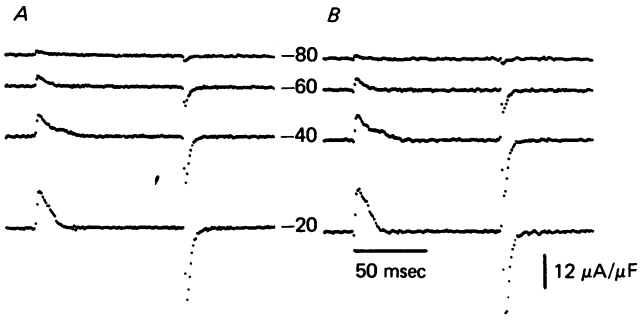

Fig. 13. Charge movement currents recorded simultaneously by the single gap and two-micro-electrode current-monitoring methods. *A*, records obtained using the standard single gap compensating circuit V_I' current-monitoring procedure. *B*, records obtained simultaneously using the two-micro-electrode ΔV current-monitoring procedure. The number next to each pair of records gives the membrane potential (mV) during the pulse. Voltage-clamp feedback was via the standard single gap compensating circuit V_m' voltage-monitoring system. Contraction was eliminated by using solution A 2 at the open end. Fibre 106, run 7. $l_C = 634$ μm, $s = 2{\cdot}13$ μm, $d = 70$ μm. Temperature 3 °C.

for the effects of λ_C in eqns. (3 A) and (8 A) assuming λ_C to be constant. Since V_2 was monitored in these experiments, the values of Q for both ΔV *and* V_I' were calculated using the complete analysis without assuming perfect voltage steps at the fibre input (see next section). The results are presented in Fig. 14. Considering all points in the figure, Q determined from ΔV was on average 14 % larger than the value determined from V_I'. The ratio of measured Qs showed no consistent variation with membrane potential. Using V_I' thus tends to underestimate Q by about the same fraction at each potential. A possible explanation for the discrepancy may be that ΔV monitors current only from the fully polarized terminated segment, whereas V_I' may monitor some current from partially depolarized membrane in the gap. The latter may have partially inactivated charge movement (Chandler *et al.* 1976*b*; Horowicz & Schneider, 1981) and thus contribute relatively more linear than non-linear capacitative charge compared with the fully polarized membrane.

Errors due to assuming perfect voltage steps at fibre input

When the compensating circuit could not be perfectly adjusted, the true potential at the start of the terminated segment rose more slowly than the controlled V_m' signal (cf. Fig. 5*b* in Kovács & Schneider, 1978) so that $V_m'(t)$ was not a perfect step. For

such 'non-square' voltage steps the analysis in the Appendix shows that our standard method of calculating transient charge, which assumes a perfect voltage step, would underestimate the true value of Q by an amount given by the second term in eqn. (2A). Since the V_2 micro-electrode was inserted just beyond the gap, micro-electrode recording provided a means of determining the error.

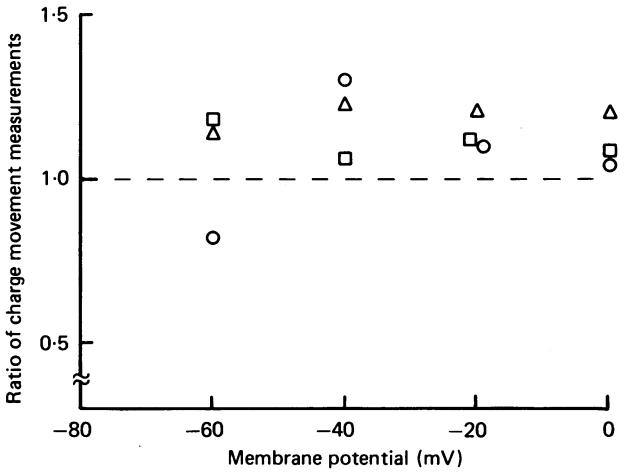

Fig. 14. Ratios of the charge movement recorded using the two-micro-electrode method to the charge movement recorded simultaneously using the single gap method. Values are plotted as a function of membrane potential during the pulse. For two fibres (100 and 103) the voltage step recorded by V_2 was not perfectly square. For each of these fibres the charge transfer due to 'non-square' voltage was added to the standard ΔV or V_I' value for both the 'mean linear' transient and non-linear transient before determining the ratios presented (see text for details). For fibre 106, the compensation was perfect and the correction for non-square voltage was negligible. Triangles: fibre 106, average results from runs 3 and 7 (see Fig. 14); circles: fibre 100, run 6 ($l_C = 730\,\mu$m, $s = 2{\cdot}81\,\mu$m, $d = 51\,\mu$m; temperature 3 °C); squares; fibre 103, run 6 ($l_C = 761\,\mu$m, $s = 2{\cdot}59\,\mu$m, $d = 78\,\mu$m; temperature 2 °C.

Assuming V_I' to be proportional to I and using V_2 for V_m, the effect of ignoring the charge transfer contributed by non-square voltage steps was evaluated at several potentials in four fibres in which V_2 was monitored and found to rise more slowly than a perfect step. Non-linear Q values were calculated for each depolarizing pulse using the standard transient charge analysis (eqn. 5A) and also using the complete analysis including charge transfer due to non-square V_2 voltage steps (eqn. 2A). Average values of the ratios of normalized Q calculated by the complete analysis to normalized Q calculated by the standard analysis are presented in Fig. 15. On average the complete analysis gave 6–8 % less charge than the values obtained with the standard analysis for the same pulse. The fact that Q was decreased when charge due to non-square voltage was included shows that the linear capacitance must have been underestimated relatively more than the non-linear component in the standard analysis. An important point concerning Fig. 15 is that the relative error in Q due to ignoring non-square voltages is not only quite small but also independent of membrane potential.

The general conclusion from this and the preceding analysis of micro-electrode measurements is that the Q calculated by the standard procedure using V_I' current recording may on average underestimate the true value of Q by between about 14 and about 7 %, depending on whether the compensation was respectively perfect or not. However, no systematic variation in the relative error in Q with pulse size appeared to be introduced using V_I'. The time course of I_Q also appeared to be faithfully recorded by the V_I' procedure.

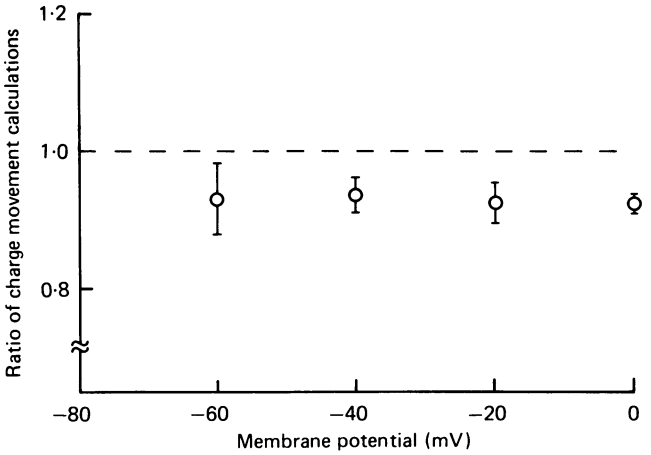

Fig. 15. Ratios of the charge movement calculated considering voltage time course at the start of the terminated fibre segment to the charge movement calculated assuming a perfectly square voltage step at the same point. Currents were first monitored using the compensating circuit with no micro-electrode in the fibre. Voltages were monitored in a subsequent run after inserting one or two micro-electrodes. Linear and non-linear charge transfers were both calculated by eqn. (2 A) with $V_m = V_2$ and $I = V_I'$ when the voltage time course was considered and by eqn. (5 A) when the voltage step was assumed to be perfectly square. Each symbol gives the mean (±1 S.E.M.) of ratios from four fibres for pulses to the indicated membrane potentials. Contraction was eliminated by solution A 2 at the open end. $482 \leqslant l_C \leqslant 761$ μm, $2{\cdot}38 \leqslant s \leqslant 2{\cdot}81$ μm, $51 \leqslant d \leqslant 78$ μm. Temperature 2 °C.

Longitudinal voltage uniformity and fibre space constants in the terminated segment

The two-micro-electrode experiments provided an opportunity to evaluate the uniformity of voltage over the terminated segment. Table 3 presents values of $\Delta V/V_1$ obtained from six fibres having terminated segment lengths l_C ranging from 482 to 762 μm. By cable theory the voltage decrement from V_1 to the end of the fibre is less than the decrement from V_2 to V_1, so that the overall fractional voltage non-uniformity over each terminated segment must have been less than twice the $\Delta V/V_1$ value in Table 3. It should also be noted that the micro-electrode impalements sometimes produced increases in current, indicating leakage conductances at the impalement sites. This effect was generally more prominent in the case of the V_1 electrode. Since leak conductances at the V_1 impalement site tend to increase $\Delta V/V_1$, the $\Delta V/V_1$ values in Table 3 presumably over-estimate the actual values for standard experiments carried out by gap recording without any electrode penetrations in the middle of the

fibre. Steady-state voltage non-uniformity along the terminated segment thus appears to have been minimal in the standard charge movement experiments.

The $\Delta V/V_1$ and l_C values for each fibre were used to calculate its space constant λ_C in the terminated segment according to the equation

$$\lambda_C = l_C\,(3V_1/8\Delta V)^{\frac{1}{2}} \tag{2}$$

TABLE 3

(1) Fibre	(2) d (μm)	(3) l_C(μm)	(4) $\Delta V/V_1$	(5) λ_C (mm)*
97	52	639	0·023†	2·6
98	52	482	0·030†	1·7
100	51	730	0·053	1·9
102	68	762	0·128	1·3
103	78	761	0·047	2·1
106	70	634	0·030	2·2
Mean	62	668	0·052	2·0
±S.E.	±5	±44	±0·016	±0·2

* These values are uncorrected for leak conductances at the V_1 electrode impalement site and are thus lower bounds on λ_C.

† These values were calculated as $\Delta V/(V'_m - \Delta V)$, since V_2 was not separately monitored.

(Adrian *et al.* 1970). Since the $\Delta V/V_1$ values are over-estimates of the values that would have been obtained in the absence of impalement leak conductances at V_1, the λ_C values in Table 3 underestimate the true fibre space constants.

Assuming the actual value of λ_C to have been greater than 2 mm in all fibres, eqn. (3A) shows that in fibres shorter than 750 mm the measured charge Q was at least 91 % of the charge Q^* which would have been required for a uniform change in potential all along the terminated segment. For larger values of λ_C or smaller maximum fibre lengths Q/Q^* would have fallen within an even smaller range below unity.

DISCUSSION

Validity of gap-recorded charge movements

The results presented here establish that the single gap method can be used to monitor reliably membrane charge movement. Using gap voltage-clamped fibres in which contraction had been eliminated by relatively high levels of internal EGTA, gap-recorded charge movements faithfully reproduced the charge movement time courses recorded simultaneously by micro-electrodes. Average Q values obtained by gap recording and the routine procedure for calculating I_Q and Q, which assumed a perfect voltage step at the input to the terminated segment, were 86 or 93 % of those that would have been obtained by a complete analysis of two-micro-electrode recordings, depending on whether the voltage step was respectively perfect or not. Both percentages were independent of membrane potential.

The single gap method also faithfully monitored charge movement in fibres with relatively low internal EGTA and maintained contractile activity. For depolarizing pulses to at most 0 mV contraction artifacts were apparently confined to a 'bowing'

in the OFF base lines of I_Q current records. They were not detectable in the ON portions of I_Q currents, provided the larger depolarizations were limited to 50 msec durations. The virtual identity of the average Q *vs.* V curves obtained from fibres with and without blocking of contraction by internal EGTA further indicates that I_Q can be reliably monitored by gap recording in contracting fibres, even for pulses producing relatively large fibre movements.

The latter finding together with the similarity of the I_Q time courses before and after blocking contraction with internal EGTA indicate that internal EGTA can eliminate contraction without any appreciable effect on membrane charge movement. In contrast, there is some evidence that hypertonic solutions, which have generally been used to block contraction for micro-electrode measurements on intact fibres, shift and perhaps steepen the Q *vs.* V relationship (see below). There are also indications that tetracaine, an agent recently used to block contraction for charge movement measurements on intact fibres, may slightly shift the Q *vs.* V relationship (Almers & Best, 1976; Almers, 1976) and may alter the I_Q kinetics (R. H. Adrian, personal communication). It thus seems that of the present procedures for blocking contraction, elevated internal EGTA may have the least effect on charge movements.

Comparison of Q vs. V *curve with results from intact fibres*

The parameter values obtained by fitting eqn. (1) to the Q *vs.* V results from cut fibres are generally consistent with the values reported for intact fibres, which are summarized in Table 4. The values are grouped according to whether hypertonicity was used to eliminate contraction or whether the experiments were carried out under isotonic conditions. In the latter case either contraction was maintained and only the initial portion of the Q *vs.* V relationship could be obtained (Schneider & Chandler, 1976; Almers, 1976) or contraction was eliminated by applying tetracaine (Almers & Best, 1976; Almers, 1976). The present Q_{max} value falls within the range of values for intact fibres, which appears to be about the same under hypertonic and isotonic conditions. Excluding the results in tetracaine, which has been shown to produce a slight positive shift in the Q *vs.* V relationship (Almers, 1976), the intact fibre results indicate that $\overline{V}$ may be more positive in isotonic solutions than in hypertonic solutions. The present $\overline{V}$ value lies between the intact fibre $\overline{V}$ values for hypertonic solutions and those estimated for isotonic solutions. The present k value falls at the upper extreme of the k estimates for intact fibres under isotonic conditions, which in turn tend to be slightly larger than the k values obtained in hypertonic solutions. The Q *vs.* V relationship measured in cut fibres, which appears to be the same with or without elimination of contraction by internal EGTA, is thus not inconsistent with the Q *vs.* V relationships estimated for intact fibres with maintained contractile activity.

Influence of ionic currents on charge measurements and contractile activation

In previous charge movement experiments on intact fibres it was observed that Q_{ON} and Q_{OFF} were no longer equal for pulses to beyond about 0 mV (Chandler *et al.* 1976*a*; Adrian & Almers, 1976; Almers & Best, 1976). This charge inequality had been attributed to residual potassium conductance activation. Since internal caesium blocks outward potassium current in nerve (Chandler & Meves, 1965; Bezanilla &

TABLE 4. Average parameter values obtained from fits to Q *vs.* V results from fully polarized fibres

Q_{max} (nC/μF)	$\overline{V}$ (mV)	k (mV)	n	Predominant cation	Predominant anion	Contraction blocker	Reference
				Hypertonic solutions			
—	−49	11	5	TEA	Cl	Hypertonicity	Schneider & Chandler (1973)
25±2	−44±3	8±1	6	TEA	Cl	Hypertonicity	Chandler *et al.* (1976*a*)
32±3	−49±3	13±2	7	TEA	SO_4	Hypertonicity	Adrian & Almers (1976)
31±2	−36±2	9±1	7	TEA	Glucuronate, Cl or SO_4	Hypertonicity	Shlevin (1979)
				Isotonic solutions			
(25)*	−27±3*	13±1	6	Na or TEA	Cl	None	Schneider & Chandler (1976)
(29)* or (37)*	−26±1* or −19±1*	15±1* or 16±1*	6	Na	SO_4	None	Almers (1976)
(29)* or 37±3	−22±1* or −14±1	12±1* or 15±1	5	Na	SO_4	Tetracaine	Almers (1976)
29±2	−27±3	13±1	4	TEA	SO_4	Tetracaine	Almers & Best (1976)
26±2	−35±1	16±1	18	TEA	SO_4	EGTA	This paper

All results were obtained using fibres from *Rana temporaria*, except those of Shlevin and the present paper which were obtained using *Rana pipiens*.

* Q_{max} was assumed, and used to calculate the other asterisked parameter(s) since only the initial part of the Q *vs.* V curve could be obtained in the presence of maintained contractile activity.

Armstrong, 1972; Dubois & Bergman, 1975), it was anticipated that in the present experiments on cut muscle fibres exposed to potassium-free caesium solutions at their open ends, outward currents through potassium channels should have been blocked. As in previous experiments on intact fibres, the external monovalent cations used in the present experiments were all impermeant and should thus have carried negligible inward current. However, it was still observed that Q_{OFF} exceeded Q_{ON} for depolarizations to and beyond 0 mV, that the excess Q_{OFF} increased with both pulse duration and pulse amplitude and that adding 20 mM-cobalt to the external solution eliminated the charge inequality without affecting Q_{ON}. It thus appears that inward ionic current tails were contaminating Q_{OFF} for depolarizations to and beyond about 0 mV. The only likely inward current carrier seems to be calcium, which would be consistent with the cobalt effect (Beaty & Stefani, 1976; Stanfield, 1977; Sanchez & Stefani, 1978).

The experiments on the growth of Q_{OFF} with the ON pulse duration provide a rather sensitive index of possible fast calcium tail currents. The results indicate that at 1–3 °C pulses to about −20 mV can produce large contractions with no detectable rapid calcium current tail. This is consistent with earlier evidence showing that calcium entry into a fibre from the external solution is not involved in excitation–contraction coupling (Armstrong, Bezanilla & Horowicz, 1972). For pulses to about 0 mV the increase in Q_{OFF} developed slowly and was very small for the 50 msec pulse durations used routinely with such pulses. Calcium entry should thus play no role in studies of the relationship between charge movement and the durations of pulses to between about −50 and 0 mV which produced just-detectable contraction, which are presented in the following paper (Horowicz & Schneider, 1981).

APPENDIX

Theory for transient charge analyses

This appendix presents the theoretical basis and underlying assumptions for making measurements of capacitative charge transfer using the single gap method. Although many of the equations have been previously derived, they are given here in rearranged form so as to be more conveniently applied to the present experimental situation. A brief treatment of analogous equations for the two-microelectrode current-monitoring method is also presented.

Single gap recording

In the present experiments a voltage change which eventually reached a steady level $V_m(\infty)$ was applied at the input of the terminated segment. The charge Q carried by the transient current entering the terminated segment during such a voltage change is conveniently defined as

$$Q = \int_0^\infty [I(t) - V_m(t)\, G]\, dt \qquad (1\,A)$$

(Adrian, Almers & Chandler, 1974). $I(t)$ and $V_m(t)$ give the time courses of current and voltage changes at the input to the terminated segment and G is the terminated segment's input conductance, which is assumed to be independent of voltage and

time. Since G is given by the ratio $I(\infty)/V_m(\infty)$ of steady current to steady voltage, the definition of Q can be re-expressed as

$$Q = \int_0^\infty [I(t) - I(\infty)]\,dt - \frac{I(\infty)}{V_m(\infty)} \int_0^\infty [V_m(t) - V_m(\infty)]\,dt. \tag{2 A}$$

This is a convenient expression for evaluating the error in Q introduced by assuming V_m to be a perfectly square voltage step (below), since the value of the second integral depends only on the input voltage relative to its steady level whereas the value of the first integral depends only on the input current relative to its steady level. Thus, for a perfect voltage step at the input to the terminated segment, the second term in eqn. (2 A) would vanish. If the input voltage were to go to $V_m(\infty)$ more slowly than as a perfect step, the second term in eqn. (2 A) would contribute positively to Q for positive values of $V_m(\infty)$ and negatively for negative ones.

The parameter which we hope to approximate by measuring Q is the capacitative charge Q^* which would be needed to change the potential by $V_m(\infty)$ uniformly over the entire terminated segment. The closeness of Q to Q^* depends on the degree of voltage decrement along the segment, which is determined by the ratio of the terminated segments length l_C to its space constant λ_C. The relationship between Q and Q^* is

$$Q^* = Q \frac{2l_C/\lambda_C}{\tanh(l_C/\lambda_C)} \left[1 + \frac{l_C/\lambda_C}{\cosh(l_C/\lambda_C)\sinh(l_C/\lambda_C)}\right]^{-1} \tag{3 A}$$

(Adrian *et al.* 1974; note that their eqn. (22 A) uses Q to refer to the transient charge applied at the middle of a fibre, one half entering each half-fibre). As l_C/λ_C approaches zero, Q approaches Q^*.

Eqns. (1 A) to (3 A) are independent of the time course of V_m and assume only that the circuit elements are linear in the terminated segment. Several additional assumptions were, however, employed in the procedure routinely used to calculate Q for these experiments. First, it was assumed that $V_m(t)$ was a perfectly square voltage step of $V_m(\infty)$ starting at $t = 0$ so that

$$Q = \int_0^\infty [I(t) - I(\infty)]\,dt. \tag{4 A}$$

Secondly, $V_I'(t)$ was assumed to be proportional to $I(t)$ (Kovács & Schneider, 1978) so that eqn. (4 A) could be expressed as

$$Q \propto \int_0^\infty [V_I'(t) - V_I'(\infty)]\,dt. \tag{5 A}$$

Thirdly, any small time-dependent current components which changed slowly during the ON or OFF intervals were assumed to be due to slow conductance changes and were removed together with the steady ionic current $V_I'(\infty)$ by subtracting straight sloping base lines from each ON and OFF V_I' record. Assuming that subtraction of sloping base lines properly removed all time-dependent ionic current, the integral in eqn. (5 A) is equal to the area under the corrected V_I' record.

In all of the above equations Q and Q^* could refer to charges transferred by either

over-all currents or currents from which the linear capacitance current had been subtracted. In the latter case, and in the absence of contaminating transient ionic currents, Q and Q^* would give the charge transferred by membrane charge movement. The procedure used to remove linear capacitative current is described in detail in the Results.

Two-micro-electrode current recording

With the two-micro-electrode method for monitoring current, $2\Delta V/r_i l_C$ approximates the internal current midway between micro-electrodes (Adrian *et al.* 1970). For this case a definition of Q which is analogous to eqn. (2 A) is

$$Q = \frac{2}{r_i l_C}\int_0^\infty [\Delta V(t) - \Delta V(\infty)]\,dt - \frac{2\Delta V(\infty)}{r_i l_C V_1(\infty)}\int_0^\infty [V_1(t) - V_1(\infty)]\,dt \qquad (6\,A)$$

(Schneider & Chandler, 1976). Using $V_2 - \Delta V$ for V_1, eqn. (6 A) can be rearranged as

$$Q = \frac{2V_2(\infty)}{r_i l_C V_1(\infty)}\int_0^\infty [\Delta V(t) - \Delta V(\infty)]\,dt - \frac{2\Delta V(\infty)}{r_i l_C V_1(\infty)}\int_0^\infty [V_2(t) - V_2(\infty)]\,dt. \qquad (7\,A)$$

Electrode 2 was inserted just beyond the gap so that V_2 was equal to V_m. Eqn. (7 A) is thus similar to eqn. (2 A) in having one integral which depends only on the current, here given by ΔV, relative to its steady level, and another which depends only on the input voltage relative to its steady level.

The relationship between the Q defined by eqns. (6 A) or (7 A) and the capacitative charge Q^* which would be required to change uniformly the potential by $V_1(\infty)$ over the final three quarters of a terminated segment composed of linear elements is

$$Q^* = Qh\{l_C/2\lambda_C\}, \qquad (8\,A)$$

where $h\{l_C/2\lambda_C\}$ is a previously defined correction factor (Schneider & Chandler, 1976).

Assuming a perfect voltage step at the input to the terminated segment the second term in eqn. (7 A) would be zero and Q would be given by

$$Q = \frac{2V_2(\infty)}{r_i l_C V_1(\infty)}\int_0^\infty [\Delta V(t) - \Delta V(\infty)]\,dt. \qquad (9\,A)$$

We thank Lic. Eduardo Ríos for helping with some of the data analyses and Ms Wendy Keck for co-ordinating the manuscript preparation. This work was supported by grants from the P.H.S. (R.C.D.A. grant K04-NS00078 to M.F.S. and R01-NS13842) and by a grant from the Muscular Dystrophy Association.

REFERENCES

ADRIAN, R. H. & ALMERS, W. (1976). Charge movement in the membrane of striated muscle. *J. Physiol.* **254**, 339–360.

ADRIAN, R. H., ALMERS, W. & CHANDLER, W. K. (1974). Appendix to ADRIAN, R. H. & ALMERS, W., Membrane capacity measurements on frog skeletal muscle in media of low ion content. *J. Physiol.* **237**, 573–606.

ADRIAN, R. H., CHANDLER, W. K. & HODGKIN, A. L. (1970). Voltage clamp experiment in striated muscle fibres. *J. Physiol.* **208**, 607–644.

ADRIAN, R. H., CHANDLER, W. K. & RAKOWSKI, R. F. (1976). Charge movement and mechanical repriming in striated muscle. *J. Physiol.* **254**, 361–388.

ADRIAN, R. H. & PERES, A. R. (1977). A gating signal for the potassium channel? *Nature, Lond.* **267**, 800–804.

ALMERS, W. (1976). Differential effects of tetracaine on delayed potassium channels and displacement currents in frog skeletal muscle. *J. Physiol.* **262**, 613–637.

ALMERS, W., ADRIAN, R. H. & LEVINSON, S. R. (1975). Some dielectric properties of muscle membrane and their possible importance for excitation–contraction coupling. *Ann. N.Y. Acad. Sci.* **264**, 278–292.

ALMERS, W. & BEST, P. M. (1976). Effects of tetracaine on displacement currents and contraction of frog skeletal muscle. *J. Physiol.* **262**, 583–611.

ARMSTRONG, C. M., BEZANILLA, F. & HOROWICZ, P. (1972). Twitches in the presence of ethylene glycol bis(β-aminoethyl ether)-*N*,*N*′-tetraacetic acid. *Biochim. biophys. Acta* **267**, 605–608.

BEATY, G. N. & STEFANI, E. (1976). Calcium dependent electrical activity in twitch muscle fibres of the frog. *Proc. R. Soc.* B **194**, 141–150.

BEZANILLA, F. & ARMSTRONG, C. M. (1972). Negative conductance caused by entry of sodium and cesium ions into the potassium channels of squid axons. *J. gen. Physiol.* **60**, 588–608.

CHANDLER, W. K. & MEVES, H. (1965). Voltage clamp experiments on internally perfused squid axons. *J. Physiol.* **180**, 788–820.

CHANDLER, W. K., RAKOWSKI, R. F. & SCHNEIDER, M. F. (1976*a*). A non-linear voltage dependent charge movement in frog skeletal muscle. *J. Physiol.* **254**, 245–283.

CHANDLER, W. K., RAKOWSKI, R. F. & SCHNEIDER, M. F. (1976*b*). Effects of glycerol treatment and maintained depolarization on charge movement in skeletal muscle. *J. Physiol.* **254**, 285–316.

CLELAND, W. W. (1967). The statistical analysis of enzyme kinetic data. *Adv. Enzymol.* **29**, 1–32.

DUBOIS, J. M. & BERGMAN, C. (1975). Cesium induced rectifications in frog myelinated fibers. *Pflügers Arch.* **355**, 361–364.

HODGKIN, A. L. & HOROWICZ, P. (1960). Potassium contractures in single muscle fibres. *J. Physiol.* **153**, 386–403.

HOROWICZ, P. & SCHNEIDER, M. F. (1981). Membrane charge moved at contraction thresholds in skeletal muscle fibres. *J. Physiol.* **314**, 595–633.

KOVÁCS, L. & SCHNEIDER, M. F. (1978). Contractile activation by voltage clamp depolarization of cut skeletal muscle fibres. *J. Physiol.* **277**, 483–506.

SANCHEZ, J. A. & STEFANI, E. (1978). Inward calcium current in twitch muscle fibres of the frog. *J. Physiol.* **283**, 197–209.

SCARBOROUGH, J. B. (1966). *Numerical Mathematical Analysis*, 6th edn. Baltimore: Johns Hopkins Press.

SCHNEIDER, M. F. & CHANDLER, W. K. (1973). Voltage dependent charge movement in skeletal muscle: a possible step in excitation–contraction coupling. *Nature, Lond.* **242**, 244–246.

SCHNEIDER, M. F. & CHANDLER, W. K. (1976). Effects of membrane potential on the capacitance of skeletal muscle fibres. *J. gen. Physiol.* **67**, 125–163.

SCHNEIDER, M. F. & HOROWICZ, P. (1977). Intramembrane charge movement and muscle contraction. *Proc. Int. Union Physiol. Sci.* **13**, 672.

SCHNEIDER, M. F. & HOROWICZ, P. (1978). Intramembrane charge movement and muscle contraction. In *Abstracts of Papers, 144th National Meeting of AAAS* (AAAS Publ. 78-2), p. 41.

SCHNEIDER, M. F. & HOROWICZ, P. (1979). Membrane charge movement at contraction thresholds in skeletal muscle. *Biophys. J.* **25**, 201a.

SHLEVIN, H. H. (1979). Effects of external calcium concentration and pH on charge movement in frog skeletal muscle. *J. Physiol.* **288**, 129–158.

STANFIELD, P. R. (1977). A calcium dependent inward current in frog skeletal muscle fibres. *Pflügers Arch.* **368**, 267–270.

VALDIOSERA, R., CLAUSEN, C. & EISENBERG, R. S. (1974). Measurements of the impedance of frog skeletal muscle fibers. *Biophys. J.* **14**, 295–315.